

The L- α -lysophosphatidylinositol/*GPR55* system and its potential role in human obesity

short running title: L- α -lysophosphatidylinositol/*GPR55* and obesity

José María Moreno-Navarrete¹, Victoria Catalán², Lauren Whyte³, Adenis Díaz-Arteaga⁴, Rafael Vázquez-Martínez⁵, Fernando Rotellar², Rocío Guzmán⁵, Javier Gómez-Ambrosi², Marina R. Pulido⁵, Wendy R. Russell⁶, Mónica Imbernón⁴, Ruth A. Ross³, María M. Malagón⁵, Carlos Dieguez⁴, José Manuel Fernández-Real¹, Gema Frühbeck² and Ruben Nogueiras⁴.

¹ Department of Diabetes, Endocrinology and Nutrition, Institut d'Investigació Biomèdica de Girona (IdIBGi) Catalonia; CIBER Fisiopatología de la Obesidad y Nutrición (CIBERObn), Spain

² Metabolic Research Laboratory, Clínica Universidad de Navarra, University of Navarra, Pamplona; CIBER Fisiopatología de la Obesidad y Nutrición (CIBERObn), Spain

³ Institute of Medical Sciences, University of Aberdeen, Aberdeen, AB25 2ZD, Scotland, UK.

⁴ Department of Physiology, School of Medicine, University of Santiago de Compostela-Instituto de Investigación Sanitaria, Santiago de Compostela; CIBER Fisiopatología de la Obesidad y Nutrición (CIBERObn), Spain

⁵ Department of Cell Biology, Physiology and Immunology, Instituto Maimónides de Investigaciones Biomédicas de Córdoba (IMIBIC), University of Córdoba, Spain.

⁶Rowett Institute of Nutrition and Health, University of Aberdeen, Aberdeen AB21 9SB, UK.

word count: **3986** / number of tables: **3** / number of figures: **5**

Address correspondence to:

Ruben Nogueiras, PhD.

Department of Physiology, School of Medicine, University of Santiago de Compostela-Instituto de Investigación Sanitaria & CIBER Fisiopatología de la Obesidad y Nutrición (CIBERObn)

S. Francisco s/n, 15782, Santiago de Compostela (A Coruña), Spain

Phone.: 34 981 582658

Fax: 34 981 574145

Email: ruben.nogueiras@usc.es

Abstract

Objective: *GPR55* is a putative cannabinoid receptor and lysophosphatidylinositol (LPI) is its only known endogenous ligand. We investigated a) whether *GPR55* is expressed in metabolically relevant human tissues (visceral fat, subcutaneous fat and liver); b) the correlation of both *GPR55* and LPI with several metabolic parameters in lean and obese subjects; and c) the actions of LPI on human adipocytes.

Research Design and Methods: We analyzed *CB1*, *CB2* and *GPR55* gene expression in adipose tissue and liver, and circulating LPI levels were measured by HPLC in 2 independent cohorts (n=95 and n=64) of obese and lean subjects, with both normal or impaired glucose tolerance and type 2 diabetes. *Ex-vivo* experiments incubating subcutaneous and visceral adipose tissue explants or isolated adipocytes with LPI were used to measure intracellular calcium and lipid accumulation.

Results: *GPR55* levels were augmented in the adipose tissue of obese subjects, and further so in obese patients with type 2 diabetes when compared with non-obese subjects. Visceral adipose tissue *GPR55* correlated positively with weight, BMI, and percent fat mass, particularly in women. On the contrary, hepatic *GPR55* gene expression was similar in obese and type 2 diabetic subjects. Circulating LPI levels were increased in obese patients and correlated with fat percentage and BMI in women. *Ex-vivo* findings indicated that LPI increased the expression of genes stimulating fat accumulation in visceral adipose tissue explants and intracellular calcium in differentiated visceral adipocytes.

Conclusions: The L- α -lysophosphatidylinositol/*GPR55* system is positively associated with obesity in humans, supporting it as a novel metabolic target of clinical relevance.

In addition to its ability to store triacylglycerol, adipocytes act as endocrine secretory cells (1). A growing number of adipocyte-derived factors have been described and their contribution to the pathophysiology of the metabolic syndrome is being investigated (2). Patients with type 2 diabetes exhibit increased activity of the endocannabinoid system in visceral fat and higher concentrations of endocannabinoids in the blood, when compared with corresponding controls (3-6). The endocannabinoid system acts through the type 1 and 2 cannabinoid receptors (*CB1* and *CB2*) (4; 7; 8). *GPR55* is a seven-transmembrane G protein-coupled receptor that shares only 13.5% sequence identity with the *CB1* receptor and 14.4% with the *CB2* receptor (9). The differences between their sequences are in agreement with the distinct relative affinities of ligands established for *CB1* or *CB2* receptors and *GPR55*.

The pharmacology of *GPR55* has provided intricate results (9-13), and a recent paper suggests that LPI has *GPR55*-independent actions in endothelial cells (14). However, it is generally accepted that LPI is an endogenous ligand of *GPR55* (15-18), since stimulation of this receptor upon LPI treatment evokes an intracellular calcium rise in several cell types. LPI belongs to the class of lysophospholipids and is generated by phosphatidylinositol hydrolysis via the action of the calcium-dependent phospholipase A2 (19) and calcium-independent phospholipase A1 (20). LPI is involved in numerous physiological actions including reproduction, angiogenesis, apoptosis, and inflammation among others (21), which are closely related to adipose tissue biology.

Most studies on the pharmacological properties of *GPR55* have used HEK293 cells transfected with *GPR55*. However, despite its wide distribution (22; 23), the physiological function of *GPR55 in vivo* remains largely unknown. Recent reports have

indicated that *GPR55* plays an important role in inflammatory pain (24), in the regulation of bone physiology by regulating osteoclast number and functions as well as bone turnover *in vivo* (17) and the LPI/*GPR55* system has been also involved in cancer (12). To our knowledge, there are no available data on the expression of *GPR55* in human tissues, or the possible involvement of LPI in energy homeostasis.

Herein, we sought to investigate the potential role of the LPI/*GPR55* system in human adiposity. We demonstrate for the first time that *GPR55* is present in human visceral and subcutaneous adipose tissue, as well as in the liver. Importantly, *GPR55* expression in visceral adipose tissue was positively associated with obesity and type 2 diabetes. Consistently, plasma LPI levels were higher in obese patients in comparison to lean subjects. *Ex-vivo* studies using both adipose tissue explants and differentiated primary adipocytes showed that LPI increased the expression of genes stimulating fat deposition in visceral adipose tissue explants. Furthermore, in differentiated adipocytes from visceral fat of obese patients, LPI raised intracellular calcium levels ($[Ca^{2+}]_i$).

Patients and Methods

Cohort 1

95 Caucasian subjects were recruited from healthy volunteers and patients attending the Departments of Endocrinology and Surgery at the Clínica Universidad de Navarra. Patients underwent a clinical assessment including medical history, physical examination, body composition analysis and co-morbidity evaluation. Obesity was classified according to BMI (>30 kg/m²). Body fat was estimated by air-displacement-plethysmography (Bod-Pod®, Life Measurements, Concord, CA) (25). Obese patients

were further subclassified according to the established diagnostic thresholds for diabetes [normoglycemia (NGT): fasting plasma glucose (FPG) concentration < 100 mg/dL and PG < 140 mg/dL 2-h after an oral glucose tolerance test (OGTT), impaired glucose tolerant (IGT): FPG between 100-125 mg/dL or PG between 140-199 mg/dL 2-h after an OGTT and type 2 diabetes: FPG > 126 mg/dL or PG \geq 200 mg/dL 2-h after OGTT] (26). Type 2 diabetes subjects were not on insulin therapy or on medication likely to influence endogenous insulin levels.

The visceral (VAT) (68 samples) and subcutaneous (SAT) (59 samples) adipose tissue samples were collected from patients undergoing either Nissen fundoplication [for hiatus hernia repair in lean volunteers] or Roux-en-Y gastric bypass [for morbid obesity treatment in obese subjects]. Tissue samples were immediately frozen and stored at -80 °C. Hepatic gene expression levels of *GPR55* were assessed in a subgroup of subjects (n=38), from which 25 out of 38 correspond to the same individuals in whom adipose tissue samples were collected. While an intraoperative liver biopsy can be performed in obese patients undergoing bariatric surgery, this procedure is not clinically justified in lean subjects. The study was approved, from an ethical and scientific standpoint, by the Hospital's Ethical Committee responsible for research and the written informed consent of participants was obtained.

Cohort 2

VAT samples from 64 consecutive subjects (35 with normal glucose tolerance, 17 with impaired fasting glucose and 12 with type 2 diabetes) were obtained at the Endocrinology Service of the Hospital Universitari Dr. Josep Trueta (Girona, Spain). Body mass index (BMI) was between 20 and 68 kg/m². Adipose tissue samples were

obtained from visceral depots during elective surgical procedures (cholecystectomy, surgery of abdominal hernia and gastric by-pass surgery). All subjects were of Caucasian origin and reported that their body weight had been stable for at least three months before the study. Liver and renal diseases were specifically excluded by biochemical work-up. All subjects gave written informed consent after the purpose of the study was explained to them. The study was approved, from an ethical and scientific standpoint, by the Ethical Committee of the Hospital Universitari Dr. Josep Trueta (Girona, Spain). Adipose tissue samples were washed, fragmented and immediately flash-frozen in liquid nitrogen before stored at -80°C. To perform the isolation of adipocyte and SVF, non-frozen tissues were washed three to four times with phosphate-buffered saline (PBS) and suspended in an equal volume of PBS supplemented with 1% penicillin-streptomycin and 0.1% collagenase type I prewarmed to 37°C. The tissue was placed in a shaking water bath at 37°C with continuous agitation for 60 minutes and centrifuged for 5 minutes at 300 to 500g at room temperature. The supernatant, containing mature adipocytes, was recollected. The pellet was identified as the SVF cell.

Blood Assays

Plasma samples were obtained by venipuncture after an overnight fast from individuals of cohort 1. All samples were allowed to settle for 10 min at room temperature prior to centrifugation at 1300 x g for 10 min. Plasma samples were then aliquoted into siliconised eppendorfs (Sigma-Aldrich), snap frozen in liquid nitrogen and stored at -80 °C. Glucose was analyzed based on enzymatic spectrophotometric reactions by an automated analyzer (Hitachi Modular P800, Roche, Basel, Switzerland). Insulin was measured by means of an enzyme-amplified chemiluminescence assay (IMMULITE®,

Diagnostic Products Corp., Los Angeles, CA). Total cholesterol, high-density lipoprotein (HDL-cholesterol) and low-density lipoprotein (LDL-cholesterol) levels were calculated as previously described (27). High sensitivity C-reactive protein (CRP) concentrations were determined as previously described (28; 29). Leptin was measured by a double-antibody RIA method (Linco Research, Inc., St. Charles, MO). Intra- and interassay coefficients of variation were 5.0 and 4.5%, respectively.

LPI analysis

Plasma samples for the measurement of LPI were obtained by venipuncture after an overnight fast from 78 individuals of cohort 1 (Supplementary table 1). Total LPI was calculated by combining 16:0, 18:0 and 20:4 LPI measurements as previously reported (30). The LPI standards; 16:0 LPI, 18:0 LPI, 20:4 LPI and 17:0 LPA were purchased from Avanti Polar Lipids. Plasma (30 μ l) in triplicate were diluted with methanol (70 μ l) containing the internal standard (17:0 LPA) at a final concentration of 100 ng/mL. Samples were mixed thoroughly mixed and centrifuged at 10,000 \times g for 10 min at 4 °C. The supernatant was removed and stored at -80 °C prior to LC-MS analysis. Liquid chromatography separation of the phospholipids was performed on an Agilent 1100 HPLC system (Agilent Technologies, Wokingham, UK) using a Phenomenex Jupiter 150 mm \times 2 mm C18 column. The gradient used to separate the phospholipids consisted of a mobile phase where solvent A was Ammonium Acetate (1 mM) and solvent B was methanol/acetonitrile 9:1 (v/v). The gradient started at 70% B and increased linearly to 100% B over 10 min before being held at 100% for 8 min. The flow rate was 300 μ l/min with an injection volume of 5 μ l. The LC eluent was directed into, without splitting, a Q-Trap 4000 triple quadrupole mass spectrometer (Applied Biosystems, Warrington, UK) fitted with a Turbo Ion Spray™ (TIS) source. For the analysis of

phospholipids, the mass spectrometer was run in negative ion mode with the following source settings: ion spray voltage -4500 V, source temperature 400 °C, Gases 1 & 2 set at 25 V and 40 V respectively and the Curtain Gas set to 10 V. The phospholipids were quantified using multiple reactions monitoring (MRM) by comparison to purchased standards. Solutions of each analyte were prepared as described above and pumped directly into the TIS via a syringe pump. The ion transitions for each of the analytes was determined based upon their molecular ion and a strong fragment ion (which corresponded to the loss of the distinctive head group); LPI (16:0, 18:0 and 20:4; Q1 = 571.4, 599.4 and 619.4 respectively and Q2 = 241.2 for all). LPA (17:0; Q1 437.20; Q2 153.10). Calibration curves were prepared for each analyte by preparing a series of standards ranging from 2 ng/μl to 10 pg/μl and the limits of detection were within this range.

Ex-vivo experiments using subcutaneous and visceral adipose tissue explants

In ex-vivo experiments using subcutaneous and visceral adipose tissue explants minced adipose tissue were used. Samples of VAT and SAT were immediately transported to the laboratory (5-10 min). The handling of tissue was carried out under strictly aseptic conditions. The tissue was cut with scissors into small pieces (5-10 mg), and incubated in buffer plus albumin (3 ml/g of tissue) for approximately 5-30 min. After incubation, the tissue explants were centrifuged for 30 s at 400 g. Then 100 mg of minced tissue was placed into 1 ml M199 (Gibco, Invitrogen) containing 10 % fetal bovine serum (Hyclone, Thermo Fisher Scientific Inc.), 100 unit/ml penicillin (Gibco, Invitrogen), 100 μg/ml streptomycin (Gibco, Invitrogen) and incubated for 48 h in suspension culture under aseptic conditions (31). Control treatment (M199) and LPI (1 and 10 μM) were compared. **The doses were selected based on previous reports (32; 33).** After 48 h,

all samples were immediately flash-frozen in liquid nitrogen before stored at -80°C. The experiment was performed in five replicates for each adipose tissue sample and treatment. To evaluate cell integrity, lactate dehydrogenase activity released from damaged cells was analyzed by the Cytotoxicity Detection Kit (lactate dehydrogenase, LDH) (Roche Diagnostics, Mannheim, Germany) according to the manufacturer's instructions in all treatments. *FASN*, *ACCI*, *ADIPOQ*, *PPARG*, *LEP* and *GPR55* relative gene expression were analysed using TaqMan® technology suitable for relative genetic expression quantification as described below.

Effect of LPI on intracellular calcium levels ($[Ca^{2+}]_i$) in cultured differentiated adipocytes

Human stromal vascular fraction cells (SVFCs) were isolated from visceral and subcutaneous adipose tissue from obese subjects undergoing open abdominal surgery (gastrointestinal by-pass) as previously described (34). SVFCs were seeded onto 25-mm round coverslips in individual plastic plates (30.000 cells/coverslip) and grown in adipocyte medium (DMEM/F-12 [1:1] (Invitrogen, Paisley, UK), 16 µM biotin, 18 µM pantothenate, 100 µM ascorbate and antibiotic-antimycotic) supplemented with 10% newborn calf serum (NCS) at 37°C in a humidified atmosphere with 95% air: 5% CO₂. After 4 days, cultured cells were induced to differentiate with a standard differentiation medium consisting of adipocyte medium supplemented with 3% NCS, 0.5 mM 3-isobutyl-1-methylxanthine (IBMX), 0.1 µM dexamethasone, 1 µM BRL49653 and 10 µg/ml insulin. After a 3-day induction period, cells were cultured in differentiation medium lacking IBMX and BRL49653. Cultures were refed every 2 days.

At day 9, cultured differentiated adipocytes were processed for $[Ca^{2+}]_i$ measurements. Briefly, cells were loaded with 2.5 μ M Fura-2AM (Molecular Probes, Eugene, OR) and 0.02% Pluronic F127 (Molecular Probes, Eugene, OR) in phenol red-free DMEM containing 20 mM $NaHCO_3$ (pH 7.4) for 30 min at 37°C. To remove extracellular dye, cells were rinsed with phenol red-free DMEM three times. Then, coverslips with dye-loaded cells were mounted in Sykes–Moore chambers and placed on the temperature-controlled stage of a Nikon Eclipse TE2000-E fluorescence microscope (Tokyo, Japan) fitted with a Plan-Fluor 40X oil immersion objective. Cells were then sequentially epilluminated at 340- and 380-nm for 100 ms every 5 s for 8-10 min. Image acquisition was controlled using Metafluor PC software (Universal Imaging Corp., West Chester, PA) and fluorescence emission was captured at 505/510 nm before and after addition of 5 μ M LPI using a back thinned-CCD cooled digital camera (ORCA II BT; Hamamatsu Photonics, Hamamatsu, Japan) running in 1-bit mode. The response of differentiated primary adipocytes to LPI was determined after establishment of a stable image baseline. Changes in $[Ca^{2+}]_i$ were recorded as ratio of the corresponding excitation wavelengths (F340/F380). Unless otherwise indicated, all other reagents were purchased from Sigma-Aldrich.

RNA Extraction and Real-Time PCR

Adipose tissue and liver RNA isolation was performed by homogenization with an ULTRA-TURRAX® T 25 basic (IKA Werke GmbH, Staufen, Germany) using TRIzol® Reagent (Invitrogen, Barcelona, Spain). Samples were purified using the RNeasy Mini kit (Qiagen) according to the manufacturer's directions. Samples were treated with DNase I (RNase-free DNase Set, Qiagen) in order to remove any trace of genomic DNA. For first strand cDNA synthesis constant amounts of 2 μ g of total RNA

were reverse transcribed in a 40 μ L final volume using random hexamers (Roche) as primers and 400 units of M-MLV reverse transcriptase (Invitrogen, Carlsbad, CA). The transcript levels for all the genes were quantified by Real-Time PCR (7300 Real Time PCR System, Applied Biosystem, Foster City, CA). Primers and probes were designed using the software Primer Express 2.0 (Applied Biosystems) and purchased from Genosys (Sigma-Aldrich, Madrid, Spain). Primers or TaqMan® probes encompassing fragments of the areas from the extremes of two exons were designed to ensure the detection of the corresponding transcript avoiding genomic DNA amplification (Supplementary table 2). The cDNA was amplified at the following conditions: 95 °C for 10 min, followed by 45 cycles of 15 s at 95 °C and 1 min at 59 °C, using the TaqMan® Universal PCR Master Mix (Applied Biosystems). The primer and probe concentrations for gene amplification were 300 nmol/L and 200 nmol/L, respectively. All results were normalized to the levels of the cyclophilin A RNA (Applied Biosystems) and relative quantification was calculated using the $\Delta\Delta C_t$ formula (35). Relative mRNA expression was expressed as fold expression over the calibrator sample (average of gene expression corresponding to the LN or NG obese groups) as previously described (35). All samples were run in duplicate and the average values were calculated.

Western blotting

White adipose tissue was homogenized in ice-cold lysis buffer containing 50 mmol/l Tris-HCl, pH 7.5, 1 mmol/l EGTA, 1 mmol/l EDTA, 1% Triton X-100, 1 mmol/l sodium orthovanadate, 50 mmol/l sodium fluoride, 5 mmol/l sodium pyrophosphate, 0.27 mol/l sucrose, 0.1% 2-mercaptoethanol, and Complete Protease Inhibitor Cocktail (1 tablet per 50 ml)(Roche Diagnostics; Mannheim, Germany). Homogenates were

centrifuged at 13.000 g for 10 min at 4°C, supernatants were removed, and aliquots were snap frozen in liquid nitrogen. Adipose tissue lysate (40 µg) was subjected to SDS-PAGE on 8% polyacrylamide gels and electrotransferred on a PVDF membrane. Membranes were then blocked for 1 hour in TBS-Tween (TBST: 50 mmol/l Tris-HCl, pH 7.5, 0.15 mol/l NaCl and 0.1% Tween) containing 3% BSA and probed for 16 h at 4°C in TBST with the appropriate dilution of the indicated antibodies (*GPR55* (Abcam): 1:500; β -Actin (Sigma Aldrich (loading control): 1:5000), as previously described (36). Detection of proteins was performed using horseradish peroxidase-conjugated secondary antibodies and an enhanced chemiluminescence reagent (Amersham Biosciences; Little Chalfont, UK).

Statistical analysis

Statistical analyses were performed using the SPSS 12.0 software statistical package (SPSS, Chicago, IL). Unless otherwise stated, descriptive results of continuous variables are expressed as mean and SE for Gaussian variables. Variables that did not fulfil a normal distribution were logarithmically transformed for subsequent analyses. The relation between variables was analyzed by simple correlation (Pearson's test) and multiple regression analyses. ANOVA was used to compare NGT, IGT and type 2 diabetes subjects followed by pair-wise *post-hoc* tests. For $[Ca^{2+}]_i$ measurements unpaired t test was used. Levels of statistical significance were set at $P < 0.05$.

Results

The main anthropometric and biochemical characteristics of the two cohorts are shown in Table 1.

Relative GPR55, CB1 and CB2 mRNA expression in white adipose tissue

The gene expression of *GPR55* (Figure 1A), *CB1* (Figure 1B) and *CB2* (Figure 1C) was higher in the VAT of obese patients in comparison with lean subjects from cohort 1. Within obese patients, *GPR55*, *CB1* and *CB2* mRNA levels were increased in the VAT of subjects with type 2 diabetes when compared to NGT and IGT obese patients (Figure 1A-C). The expression of the three receptors was also assessed in the SAT, where we failed to detect *CB2* gene expression. The pattern of expression of *GPR55* and *CB1* was quite similar to that observed in VAT. Both, *GPR55* (Figure 1D) and *CB1* (Figure 1E) were higher in the SAT from obese diabetic patients when compared to obese NGT and IGT patients in cohort 1 subjects. Consistently with the results obtained in cohort 1, *GPR55* gene expression was increased in the VAT of obese diabetic patients when compared to obese NGT and IGT patients in cohort 2 subjects (Figure 1F). In accordance with the gene expression data, we found that *GPR55* protein levels were significantly increased in the VAT from obese patients in comparison to lean subjects (Figure 1G). Similarly to that observed for *GPR55* gene expression, the protein levels of this receptor were increased in T2D patients when compared to NGT patients (Figure 1H). Additionally, we compared *GPR55* mRNA (Figure 1I) and protein (Figure 1J) expression levels between VAT and SAT from the same individuals and found that *GPR55* levels were significantly lower in SAT. Finally, *CB1* mRNA expression was also higher in VAT when compared to SAT (Figure 1K).

In a multivariate linear regression analysis, BMI contributed to 6% of the variance in *GPR55* gene expression levels independently of age, sex and type 2 diabetes status (Supplementary table 3). The higher expression of *GPR55* in obese patients in

comparison with lean subjects from cohort 1 was in agreement with a positive correlation between VAT *GPR55* levels and body weight ($p < 0.01$) (Figure 2A), BMI (Figure 2B), circulating LPI levels (Figure 2C) and percent fat mass ($p = 0.03$) (Table 2). Given that some groups were not exactly matched for gender, an analysis was performed to verify whether the observed differences were due to gender. A correlation was constructed considering only men or women and the results showed that *GPR55* expression exhibited significantly higher levels with increasing BMI in both sexes (Table 2). On the contrary, we did not find a significant correlation between SAT *GPR55* mRNA levels with any of the variables studied (Table 2). Contrary to *GPR55*, VAT CB1 expression was not correlated to BMI (Table 3), although SAT CB1 expression showed such a correlation but only in women (Table 3).

Similarly to cohort 1, we also found that VAT *GPR55* mRNA levels were positively associated with body weight ($p = 0.01$) (Figure 2D), BMI ($p = 0.03$) (Figure 2E), and percent fat mass ($p = 0.03$) (Table 4) in the subjects of cohort 2. Thus, *GPR55* gene expression levels were increased in the VAT of obese patients in both cohorts, and the correlation of *GPR55* gene expression with weight, BMI and fat mass was especially significant in women in both cohorts (Table 2 and 4). Therefore, we can conclude that *GPR55* gene expression is specifically increased in VAT, but not SAT, of obese subjects.

Relative GPR55 mRNA expression in adipocytes vs the stromal vascular fraction (SVF)

We then studied which fraction of the adipose tissue accounted for this increased expression. In order to address this issue, we used human visceral fat and subcutaneous fat, and separated the adipocyte fraction from the SVF fraction. In visceral fat,

adipogenic genes (*FASN*, *ACC* and *SREBP*) were significantly increased in the adipocyte fraction (Supplementary Figure 1A-C), while *CD14* (monocyte marker) was significantly increased in the SVF fraction (Supplementary Figure 1D). The *GPR55* gene was similarly expressed in both the adipocyte and the SVF fractions (Supplementary Figure 1E). Similar results were obtained in SAT (data not shown).

Circulating LPI levels in lean and obese subjects

Next, we assessed plasma LPI levels, the only known endogenous ligand of *GPR55* in lean and obese subjects from cohort 1. We found that total LPI was significantly increased in obese patients in comparison with lean subjects (Figure 3A). Similarly to plasma total LPI levels, we found that all three individual LPI species measured, 16:0 LPI (Figure 3B), 18:0 LPI (Figure 3C), and 20:4 LPI (Figure 3D), were also increased in the three groups of obese patients when compared to lean volunteers with the exception of 18:0 LPI in type 2 diabetic patients.

Plasma LPI levels were not correlated with body weight or BMI when men and women were analyzed together (data not shown). However, when a correlation was constructed considering only men or women, the results showed that plasma LPI exhibited significantly higher levels with increasing body weight (Figure 3E), BMI (Figure 3F), and fat percentage (Figure 3G) in women but not men (Table 5). Finally, we also found that plasma LPI correlates with low density lipoprotein (LDL) levels in women but not men (Table 5). Importantly, circulating levels of total LPI (Figure 3H), 16:0 LPI (Figure 3I), 18:0 LPI (Figure 3J), and 20:4 LPI (Figure 3K) were not significantly different between men and women.

Effects of LPI on human adipose tissue explants

After demonstrating that VAT *GPR55* and plasma LPI correlate with obesity, we then assessed the direct effects of LPI on explants obtained from SAT and VAT. LPI (1 and 10 μM) increased the expression of genes promoting the synthesis of fatty acids including fatty acid synthase (FASN) (Figure 4A) and acetyl CoA carboxylase (ACC) in explants from VAT (Figure 4B). Both doses of LPI also triggered the expression of peroxisome proliferator-activated receptor gamma (PPARG) (Figure 4C), which plays an important role in adipocyte differentiation. Other adipokines such as leptin (Figure 4D) or adiponectin (ADIPOQ) (Figure 4E) tended to show a slight increase in their expression, but the differences were not statistically significant. The expression of *GPR55* was significantly up-regulated by LPI at both doses (Figure 4F) in adipocytes from VAT. In contrast to the findings obtained in VAT, LPI did not modify the expression of any of the studied genes in explants obtained from SAT (Figure 4G-4L).

Effects of LPI on $[\text{Ca}^{2+}]_i$ in cultured differentiated human adipocytes

LPI has previously been shown to increase $[\text{Ca}^{2+}]_i$ in HEK293 cells expressing *GPR55* (15; 16) as well as in rat pheochromocytoma PC12 cells (37). Given that increases in $[\text{Ca}^{2+}]_i$ have been associated with lipogenesis in adipocytes (38), we next analyzed whether LPI was capable to enhance $[\text{Ca}^{2+}]_i$ in cultured differentiated adipocytes obtained from SVF of VAT and SAT of obese patients. For this purpose, after a 9-day differentiation period, VAT and SAT adipocytes were loaded with the calcium sensitive probe Fura-2 AM and $[\text{Ca}^{2+}]_i$ was monitored over time (8-10 min) in the absence and presence of LPI. We found that exposure of cells to 5 μM LPI induced a substantial rise in $[\text{Ca}^{2+}]_i$ in 48.4% of differentiated VAT adipocytes (46 out of 95 cells; n= 3 independent experiments) and in 24.4% of differentiated SAT cells (29 out of 119 cells;

n= 3 independent experiments) (Figs. 5A and C, respectively). In terms of response intensity, differentiated VAT adipocytes treated with 5 μ M LPI exhibited an increase in $[Ca^{2+}]_i$ significantly higher than that observed in differentiated SAT adipocytes ($43.18\% \pm 2.77\%$ vs. $19.69\% \pm 1.93\%$ above basal levels in VAT and SAT, respectively; $P < 0.001$) (Figs. 5B and D, respectively).

Relative GPR55 mRNA expression in the liver

In addition to its expression in adipose tissue, we also found that *GPR55* is expressed in the liver. No significant differences in hepatic *GPR55* gene expression levels between NGT, IGT and type 2 diabetes obese patients were observed (Supplementary Figure 2).

Effect of LPI on adipocyte differentiation of 3T3-L1 cells

When 3T3-L1 cells were treated with LPI (1 and 10 μ M) during 10 days, we did not find any alteration in the Oil Red O staining in comparison to the control cells (Supplementary Figure 3). Thus, these results indicate that LPI acts differently in human and rodent adipocytes.

Relative GPR55 levels in the white adipose tissue of obese animals

Mice lacking leptin (Supplementary Figure 4A) and rats fed a high-fat diet (45% by energy) (Supplementary Figure 4B) showed significantly decreased *GPR55* mRNA levels in the WAT when compared to lean animals. Accordingly, *GPR55* protein levels were also decreased in both obese models (Supplementary Figures 4C and 4D). Therefore, these findings suggest that *GPR55* is differentially regulated in humans and rodents.

Discussion

The endocannabinoid system is overactive in WAT of obese patients, thereby contributing to excessive visceral fat accumulation and obesity-associated complications (4; 6; 39). *GPR55* has been described as a putative receptor for atypical cannabinoids (9; 40; 41). However, its clinical implications remain largely unknown. Herein, we demonstrate that *GPR55* is expressed in human SAT, VAT and liver. Our findings, obtained in two independent cohorts, indicate that *GPR55* mRNA levels are increased in the VAT and SAT of obese subjects in comparison to lean volunteers. Moreover, VAT but not SAT *GPR55* expression is positively associated with type 2 diabetes. Interestingly, correlations between VAT *GPR55* gene levels and weight, BMI and percentage body fat are stronger in women than in men. Consistently, plasma LPI levels are also increased in obese patients and positively correlated with weight, BMI and percentage body fat in women. Finally, we show that in explants obtained from VAT, LPI triggers the mRNA levels of genes promoting lipogenesis, and in cultured differentiated adipocytes obtained from VAT LPI raises $[Ca^{2+}]_i$. However, we found that LPI evoked minor responses in adipose tissue explants or in cultured differentiated adipocytes obtained from SAT, suggesting that the LPI/*GPR55* system is particularly important in VAT.

In rodents, *GPR55* mRNA has been detected throughout the central nervous system (22) and in peripheral tissues (23). Our study is the first to show that *GPR55* mRNA is expressed in human tissues, and its regulation is tissue-specific, because *GPR55* expression in WAT, but not liver, is particularly up-regulated in diabetic patients when compared to NGT obese individuals. Specifically, *GPR55* is found at similar concentrations in both adipocytes and the stromal vascular fraction of fat tissue,

indicating that this receptor is also present in other cell types present in the stromal vascular fraction such as mononuclear cells (monocytes, macrophages and lymphocytes) among others. The current findings are consistent with previous reports demonstrating that *GPR55* is located in human monocytes (17). In obese states, the stromal vascular fraction is largely infiltrated by mononuclear cells in comparison to normal conditions.

Although endocannabinoid levels are increased in obesity (39), data on *CBI* gene expression in WAT is controversial since reduced (39), increased (42) or unchanged (43) expression between obese and lean subjects have been reported. In the current work, we detected higher *CBI* mRNA levels in the adipose tissue of obese patients. Although the discrepancies for those differences are unknown, a plausible explanation might be the different populations used by the studies. Similarly to *CBI*, *CB2* and *GPR55* mRNA levels in the VAT of obese subjects were also increased, indicating the lack of a negative feedback loop between circulating endocannabinoids and these three cannabinoid receptors. The similar pattern of expression of the three receptors in obese and diabetic patients also suggests that some of their metabolic functions might be overlapped or compensated. This is an important issue because specific drugs for each receptor might also act through the other two receptors when the drug is administered at high doses or during long-term treatments. As a matter of fact, a recent pharmacological study suggests that low concentrations of Rimonabant specifically block *CBI* receptors, but higher doses or long-term treatment could be also targeting *GPR55* (44). Other reports carried out in HEK cells showed that the endocannabinoids anandamide and 2-arachidonoylglycerol have also a low affinity by *GPR55* (16; 23; 45). Thus, *GPR55*

activation could be contributing to the biological activity in situations wherein endocannabinoid levels are markedly increased.

Despite activation of *GPR55* by cannabinoids, it is well accepted that LPI is its more potent endogenous ligand known up to date (15-18). Plasma LPI levels have been previously found to be increased in patients with ovarian cancer, thereby considering LPI as a biomarker for this disease (30; 46; 47). However, to our knowledge, no reports have studied the interaction between LPI levels and metabolism. Similarly to *GPR55* expression, we found that plasma LPI is increased in obesity, suggesting that the LPI/*GPR55* system is overactive in obese states. It is well known that visceral fat accumulation represents a key pathophysiologic mechanism for the clustering of metabolic abnormalities, including insulin resistance and type 2 diabetes (48). We found that within obese patients, *GPR55* gene levels in VAT and SAT are significantly increased in diabetic subjects, suggesting that this receptor may play a pivotal role in the development of insulin resistance and the pathogenesis of type 2 diabetes. *GPR55* gene expression in VAT but not SAT was positively correlated with several anthropometric parameters such as body weight and BMI in the two cohorts examined. Interestingly, when men and women are analyzed separately, VAT *GPR55* shows a stronger correlation with weight, BMI and fat percentage in women. Marked gender differences have been reported with regard to degrees of insulin resistance, body composition and energy balance (49). Our results showing that VAT *GPR55* mRNA expression is correlated with weight, BMI and percentage body fat in women suggest that estrogens might be relevant to the *GPR55* signaling pathway. Importantly, the correlation of plasma LPI levels to weight, BMI and percentage body fat is almost identical to that of VAT *GPR55*, as those correlations were positive only in women but not men. This

sexual dimorphism in gene expression and circulating levels has been previously observed in other hormones with important metabolic implications such as leptin gene expression (50) or circulating leptin concentrations (51).

Since both LPI and VAT *GPR55* showed a clear up-regulation in obese patients and were correlated with important metabolic parameters, we next sought to investigate the direct actions of this system on adipose tissue explants and isolated adipocytes. Our findings indicated that in explants obtained from VAT, LPI induced lipid storage by stimulating lipogenic genes, and promoted adipocyte differentiation by increasing PPAR γ expression. Although *GPR55* was also present in SAT, the treatment of explants from SAT with LPI did not modify the expression of any of the genes studied. Consistent with the gene expression studies and the lipogenic action of [Ca²⁺]_i in adipocytes (38), LPI elicited a significantly higher effect in [Ca²⁺]_i in cultured differentiated adipocytes from VAT than in those from SAT, both in terms of percentage of responsive cells and the magnitude of the [Ca²⁺]_i increase. Indeed, although the doses of LPI tested herein were similar to others used in previous works (32; 33), they are higher than plasma concentration observed in obese patients, but overall, these results indicate that LPI directly favors a condition of lipid deposition within adipocytes from VAT. Given the specific correlations between LPI/*GPR55* and several metabolic parameters in women, further studies will be necessary to address if estrogens can interfere in the biological actions of LPI. In this sense, it is important to point out that body fat is differentially distributed in men and women, with men exhibiting more visceral fat than women, in whom subcutaneous fat predominates (49). The different distribution of fat between both sexes might have clear implications in the metabolic actions of the LPI/*GPR55* system. It is also important to point out that LPI is esterified

by the enzyme 1-acylglycerol-3-phosphate-O-acyltransferase 3 (AGPAT3), which is ubiquously expressed in human tissues (52). Thus, it is tempting to speculate that the tissue-specific actions of LPI might be explained by the distinct grade of activity of this enzyme in those fat depots.

In addition to adipose tissue, we also detected the expression of *GPR55* in the liver. However, we failed to detect significant changes in expression between the different subgroups of obese patients. Although further studies should elucidate the expression of this receptor in other tissues with metabolic functions, including the gastrointestinal tract, skeletal muscle or pancreas, our current findings suggest that VAT *GPR55* may be the most important one regarding energy homeostasis.

In summary, our findings obtained in two independent cohorts demonstrate that: 1) *GPR55* levels are increased in both VAT and SAT of obese subjects; 2) VAT *GPR55* is positively correlated with weight, BMI, and percentage body fat particularly in women; 3) hepatic *GPR55* gene expression remains unchanged in obese and diabetic subjects; 4) circulating LPI levels are increased in obesity and correlated with weight, BMI and fat percentage in women; and 5) LPI increases intracellular calcium levels and the expression of lipogenic enzymes specifically in differentiated adipocytes from VAT. This work suggests that the LPI/*GPR55* system is a new metabolic pathway of clinical relevance. Further studies are required to investigate the potential role of agonists/antagonists for *GPR55* in obesity and insulin sensitivity.

Acknowledgements

The authors gratefully acknowledge the valuable collaboration of all the members of the Multidisciplinary Obesity Team of the Clínica Universidad de Navarra, and thank Lorraine Scobbie and Gary Duthie (Rowett Institute of Nutrition and Health, Aberdeen, UK) for their excellent technical assistance. This work has been supported by grants from Ministerio de Educacion y Ciencia (RN: RYC-2008-02219; RN: SAF2009-07049; CD: BFU2008-02001, JMFR: SAF2008- 02073; MMM: BFU2010-17116), Instituto de Salud Carlos III (GF: FIS PS09/02330); Xunta de Galicia (CD: PGIDIT06PXIB208063PR); European Union (CD: Health-F2-2008-223713: “*Reprobesity*”); the research leading to these results has also received funding from the European Community's Seventh Framework Programme (FP7/2007-2013) under grant agreement n° 245009. CIBER de Fisiopatología de la Obesidad y Nutrición is an initiative of ISCIII.

J.M.M-N. researched data and contributed to discussion. V.C. researched data and contributed to discussion. L.W. researched data and contributed to discussion. A.D-A. researched data. R.V-M. researched data and contributed to discussion. F.R. researched data. R.G. researched data. J.G-A. researched data and contributed to discussion. M.P. researched data and contributed to discussion. W.R.R. researched data. M.I. researched data. R.A.R. reviewed/edited manuscript. M.M.M. reviewed/edited manuscript. C.D. reviewed/edited manuscript. J.M.F-R. reviewed/edited manuscript. G.F. reviewed/edited manuscript. R.N. wrote manuscript.

References

1. Badman MK, Flier JS: The adipocyte as an active participant in energy balance and metabolism. *Gastroenterology* 132:2103-2115, 2007
2. Fernandez-Real JM, Ricart W: Insulin resistance and chronic cardiovascular inflammatory syndrome. *Endocr Rev* 24:278-301, 2003
3. Matias I, Gonthier MP, Orlando P, Martiadis V, De Petrocellis L, Cervino C, Petrosino S, Hoareau L, Festy F, Pasquali R, Roche R, Maj M, Pagotto U, Monteleone P, Di Marzo V: Regulation, function, and dysregulation of endocannabinoids in models of adipose and beta-pancreatic cells and in obesity and hyperglycemia. *J Clin Endocrinol Metab* 91:3171-3180, 2006
4. Pagotto U, Marsicano G, Cota D, Lutz B, Pasquali R: The emerging role of the endocannabinoid system in endocrine regulation and energy balance. *Endocr Rev* 27:73-100, 2006
5. Bluher M, Engeli S, Kloting N, Berndt J, Fasshauer M, Batkai S, Pacher P, Schon MR, Jordan J, Stumvoll M: Dysregulation of the peripheral and adipose tissue endocannabinoid system in human abdominal obesity. *Diabetes* 55:3053-3060, 2006
6. Di Marzo V: The endocannabinoid system in obesity and type 2 diabetes. *Diabetologia* 51:1356-1367, 2008
7. Cota D: Role of the endocannabinoid system in energy balance regulation and obesity. *Front Horm Res* 36:135-145, 2008
8. Pagotto U, Cervino C, Vicennati V, Marsicano G, Lutz B, Pasquali R: How many sites of action for endocannabinoids to control energy metabolism? *Int J Obes (Lond)* 30 Suppl 1:S39-43, 2006
9. Ross RA: The enigmatic pharmacology of GPR55. *Trends Pharmacol Sci* 30:156-163, 2009
10. Pertwee RG: GPR55: a new member of the cannabinoid receptor clan? *Br J Pharmacol* 152:984-986, 2007
11. Petitet F, Donlan M, Michel A: GPR55 as a new cannabinoid receptor: still a long way to prove it. *Chem Biol Drug Des* 67:252-253, 2006
12. Ross RA: L-alpha-Lysophosphatidylinositol meets GPR55: a deadly relationship. *Trends Pharmacol Sci*
13. Okuno T, Yokomizo T: What is the natural ligand of GPR55? *J Biochem*
14. Bondarenko AI, Malli R, Graier WF: The GPR55 agonist lysophosphatidylinositol acts as an intracellular messenger and bidirectionally modulates Ca²⁺-activated large-conductance K⁺ channels in endothelial cells. *Pflugers Arch* 461:177-189
15. Oka S, Nakajima K, Yamashita A, Kishimoto S, Sugiura T: Identification of GPR55 as a lysophosphatidylinositol receptor. *Biochem Biophys Res Commun* 362:928-934, 2007
16. Henstridge CM, Balenga NA, Ford LA, Ross RA, Waldhoer M, Irving AJ: The GPR55 ligand L-alpha-lysophosphatidylinositol promotes RhoA-dependent Ca²⁺ signaling and NFAT activation. *FASEB J* 23:183-193, 2009
17. Whyte LS, Ryberg E, Sims NA, Ridge SA, Mackie K, Greasley PJ, Ross RA, Rogers MJ: The putative cannabinoid receptor GPR55 affects osteoclast function in vitro and bone mass in vivo. *Proc Natl Acad Sci U S A* 106:16511-16516, 2009
18. Oka S, Kimura S, Toshida T, Ota R, Yamashita A, Sugiura T: Lysophosphatidylinositol Induces Rapid Phosphorylation of p38 Mitogen-Activated Protein Kinase and Activating Transcription Factor 2 in HEK293 Cells Expressing GPR55 and IM-9 Lymphoblastoid Cells. *J Biochem*

19. Billah MM, Lapetina EG: Formation of lysophosphatidylinositol in platelets stimulated with thrombin or ionophore A23187. *J Biol Chem* 257:5196-5200, 1982
20. Kobayashi T, Kishimoto M, Okuyama H: Phospholipases involved in lysophosphatidylinositol metabolism in rat brain. *J Lipid Mediat Cell Signal* 14:33-37, 1996
21. Choi JW, Lee CW, Chun J: Biological roles of lysophospholipid receptors revealed by genetic null mice: an update. *Biochim Biophys Acta* 1781:531-539, 2008
22. Sawzdargo M, Nguyen T, Lee DK, Lynch KR, Cheng R, Heng HH, George SR, O'Dowd BF: Identification and cloning of three novel human G protein-coupled receptor genes GPR52, PsiGPR53 and GPR55: GPR55 is extensively expressed in human brain. *Brain Res Mol Brain Res* 64:193-198, 1999
23. Ryberg E, Larsson N, Sjogren S, Hjorth S, Hermansson NO, Leonova J, Elebring T, Nilsson K, Drmota T, Greasley PJ: The orphan receptor GPR55 is a novel cannabinoid receptor. *Br J Pharmacol* 152:1092-1101, 2007
24. Staton PC, Hatcher JP, Walker DJ, Morrison AD, Shapland EM, Hughes JP, Chong E, Mander PK, Green PJ, Billinton A, Fulleylove M, Lancaster HC, Smith JC, Bailey LT, Wise A, Brown AJ, Richardson JC, Chessell IP: The putative cannabinoid receptor GPR55 plays a role in mechanical hyperalgesia associated with inflammatory and neuropathic pain. *Pain* 139:225-236, 2008
25. Ginde SR, Geliebter A, Rubiano F, Silva AM, Wang J, Heshka S, Heymsfield SB: Air displacement plethysmography: validation in overweight and obese subjects. *Obes Res* 13:1232-1237, 2005
26. Genuth S, Alberti KG, Bennett P, Buse J, Defronzo R, Kahn R, Kitzmiller J, Knowler WC, Lebovitz H, Lernmark A, Nathan D, Palmer J, Rizza R, Saudek C, Shaw J, Steffes M, Stern M, Tuomilehto J, Zimmet P: Follow-up report on the diagnosis of diabetes mellitus. *Diabetes Care* 26:3160-3167, 2003
27. Catalan V, Gomez-Ambrosi J, Ramirez B, Rotellar F, Pastor C, Silva C, Rodriguez A, Gil MJ, Cienfuegos JA, Fruhbeck G: Proinflammatory cytokines in obesity: impact of type 2 diabetes mellitus and gastric bypass. *Obes Surg* 17:1464-1474, 2007
28. Gomez-Ambrosi J, Salvador J, Rotellar F, Silva C, Catalan V, Rodriguez A, Jesus Gil M, Fruhbeck G: Increased serum amyloid A concentrations in morbid obesity decrease after gastric bypass. *Obes Surg* 16:262-269, 2006
29. Gomez-Ambrosi J, Catalan V, Ramirez B, Rodriguez A, Colina I, Silva C, Rotellar F, Mugueta C, Gil MJ, Cienfuegos JA, Salvador J, Fruhbeck G: Plasma osteopontin levels and expression in adipose tissue are increased in obesity. *J Clin Endocrinol Metab* 92:3719-3727, 2007
30. Sutphen R, Xu Y, Wilbanks GD, Fiorica J, Grendys EC, Jr., LaPolla JP, Arango H, Hoffman MS, Martino M, Wakeley K, Griffin D, Blanco RW, Cantor AB, Xiao YJ, Krischer JP: Lysophospholipids are potential biomarkers of ovarian cancer. *Cancer Epidemiol Biomarkers Prev* 13:1185-1191, 2004
31. Moreno-Navarrete JM, Ortega FJ, Rodriguez-Hermosa JI, Sabater M, Pardo G, Ricart W, Fernandez-Real JM: OCT1 Expression in adipocytes could contribute to increased metformin action in obese subjects. *Diabetes* 60:168-176
32. Bondarenko A, Waldeck-Weiermair M, Naghdi S, Poteser M, Malli R, Graier WF: GPR55-dependent and -independent ion signalling in response to lysophosphatidylinositol in endothelial cells. *Br J Pharmacol* 161:308-320
33. Kapur A, Zhao P, Sharir H, Bai Y, Caron MG, Barak LS, Abood ME: Atypical responsiveness of the orphan receptor GPR55 to cannabinoid ligands. *J Biol Chem* 284:29817-29827, 2009

34. Rodriguez A, Gomez-Ambrosi J, Catalan V, Gil MJ, Becerril S, Sainz N, Silva C, Salvador J, Colina I, Fruhbeck G: Acylated and desacyl ghrelin stimulate lipid accumulation in human visceral adipocytes. *Int J Obes (Lond)* 33:541-552, 2009
35. Catalan V, Gomez-Ambrosi J, Rotellar F, Silva C, Rodriguez A, Salvador J, Gil MJ, Cienfuegos JA, Fruhbeck G: Validation of endogenous control genes in human adipose tissue: relevance to obesity and obesity-associated type 2 diabetes mellitus. *Horm Metab Res* 39:495-500, 2007
36. Velasquez DA, Martinez G, Romero A, Vazquez MJ, Boit KD, Dopeso-Reyes IG, Lopez M, Vidal A, Nogueiras R, Dieguez C: The Central Sirtuin1/p53 Pathway Is Essential for the Orexigenic Action of Ghrelin. *Diabetes*
37. Ma MT, Yeo JF, Farooqui AA, Zhang J, Chen P, Ong WY: Differential effects of lysophospholipids on exocytosis in rat PC12 cells. *J Neural Transm* 117:301-308
38. Gericke MT, Kosacka J, Koch D, Nowicki M, Schroder T, Ricken AM, Nieber K, Spanel-Borowski K: Receptors for NPY and PACAP differ in expression and activity during adipogenesis in the murine 3T3-L1 fibroblast cell line. *Br J Pharmacol* 157:620-632, 2009
39. Engeli S, Bohnke J, Feldpausch M, Gorzelniak K, Janke J, Batkai S, Pacher P, Harvey-White J, Luft FC, Sharma AM, Jordan J: Activation of the peripheral endocannabinoid system in human obesity. *Diabetes* 54:2838-2843, 2005
40. Brown AJ: Novel cannabinoid receptors. *Br J Pharmacol* 152:567-575, 2007
41. Johns DG, Behm DJ, Walker DJ, Ao Z, Shapland EM, Daniels DA, Riddick M, Dowell S, Staton PC, Green P, Shabon U, Bao W, Aiyar N, Yue TL, Brown AJ, Morrison AD, Douglas SA: The novel endocannabinoid receptor GPR55 is activated by atypical cannabinoids but does not mediate their vasodilator effects. *Br J Pharmacol* 152:825-831, 2007
42. Bensaid M, Gary-Bobo M, Esclangon A, Maffrand JP, Le Fur G, Oury-Donat F, Soubrie P: The cannabinoid CB1 receptor antagonist SR141716 increases Acrp30 mRNA expression in adipose tissue of obese fa/fa rats and in cultured adipocyte cells. *Mol Pharmacol* 63:908-914, 2003
43. Lofgren P, Sjolín E, Wahlen K, Hoffstedt J: Human adipose tissue cannabinoid receptor 1 gene expression is not related to fat cell function or adiponectin level. *J Clin Endocrinol Metab* 92:1555-1559, 2007
44. Henstridge CM, Balenga NA, Schroder R, Kargl JK, Platzer W, Martini L, Arthur S, Penman J, Whistler JL, Kostenis E, Waldhoer M, Irving AJ: GPR55 ligands promote receptor coupling to multiple signalling pathways. *Br J Pharmacol*
45. Lauckner JE, Jensen JB, Chen HY, Lu HC, Hille B, Mackie K: GPR55 is a cannabinoid receptor that increases intracellular calcium and inhibits M current. *Proc Natl Acad Sci U S A* 105:2699-2704, 2008
46. Xiao Y, Chen Y, Kennedy AW, Belinson J, Xu Y: Evaluation of plasma lysophospholipids for diagnostic significance using electrospray ionization mass spectrometry (ESI-MS) analyses. *Ann N Y Acad Sci* 905:242-259, 2000
47. Shen Z, Wu M, Elson P, Kennedy AW, Belinson J, Casey G, Xu Y: Fatty acid composition of lysophosphatidic acid and lysophosphatidylinositol in plasma from patients with ovarian cancer and other gynecological diseases. *Gynecol Oncol* 83:25-30, 2001
48. Despres JP: Is visceral obesity the cause of the metabolic syndrome? *Ann Med* 38:52-63, 2006
49. Shi H, Seeley RJ, Clegg DJ: Sexual differences in the control of energy homeostasis. *Front Neuroendocrinol* 30:396-404, 2009

50. Perica's J, Oliver P, Guitard R, Pico C, Palou A: Sexual dimorphism in age-related changes in UCP2 and leptin gene expression in subcutaneous adipose tissue in humans. *J Nutr Biochem* 12:444-449, 2001
51. Rosenbaum M, Pietrobelli A, Vasselli JR, Heymsfield SB, Leibel RL: Sexual dimorphism in circulating leptin concentrations is not accounted for by differences in adipose tissue distribution. *Int J Obes Relat Metab Disord* 25:1365-1371, 2001
52. Prasad SS, Garg A, Agarwal AK: Enzymatic activities of the human AGPAT isoform 3 and isoform 5: localization of AGPAT5 to mitochondria. *J Lipid Res* 52:451-462

Table 1. Anthropometric and analytical characteristics of subjects in cohort 1 and cohort 2.**Cohort 1**

	Lean	Obese NGT	Obese IGT	Obese T2DM	P
n (men/women)	5 (2/3)	34 (13/21)	27 (14/13)	29 (13/16)	
Age (years)	38 ± 4	38 ± 2	42 ± 2	47 ± 2 ^{††}	<0.001
BMI (kg/m²)	21.3 ± 1.1	42.7 ± 1.1 ^{**}	46.0 ± 1.2 ^{**}	47.6 ± 1.8 ^{**}	<0.001
Body fat (%)	26.5 ± 2.8	48.3 ± 1.6 ^{**}	53.3 ± 1.0 ^{**}	50.6 ± 1.5 ^{**}	<0.001
Fasting glucose (mg/dL)	86.8 ± 3.5	89.0 ± 1.7	105.2 ± 2.2	139.9 ± 10.9 ^{**††,##}	<0.001
Fasting insulin (μU/mL)	8.2 ± 1.7	17.4 ± 1.6 [*]	18.0 ± 2.3 [*]	20.2 ± 2.6 [*]	0.012
Triglycerides (mg/dL)	68 ± 11	103 ± 8	139 ± 24	191 ± 42	0.066
Cholesterol (mg/dL)	192 ± 10	181 ± 8	208 ± 8	205 ± 8	0.066
LDL-cholesterol (mg/dL)	118 ± 10	119 ± 6	130 ± 7	133 ± 8	0.443
HDL-cholesterol (mg/dL)	58 ± 2	41 ± 2 [*]	49 ± 2 [†]	42 ± 2 [*]	<0.001
Leptin (ng/mL)	7.8 ± 1.5	48.0 ± 5.4 [*]	60.8 ± 6.4 ^{**}	61.9 ± 8.5 ^{**}	0.003
CRP (mg/L)	1.8 ± 0.3	6.6 ± 1.3	12.8 ± 2.3 ^{*,†}	9.0 ± 1.5	0.011
AUC glucose		15.7 ± 0.6	20.3 ± 0.6 ^{†††}	26.2 ± 1.5 ^{†††}	0.001
AUC insulin		13.0 ± 1.4	11.8 ± 1.2	7.6 ± 1.3	0.055
2h-glucose (OGTT)		108.5 ± 2.6	168.2 ± 3.7 ^{†††}	247.7 ± 24.1 ^{†††}	<0.001
HOMA-IR	1.7 ± 0.3	4.8 ± 0.7	4.7 ± 0.6	7.1 ± 1.3 [†]	<0.05

Cohort 2

	Obese NGT	Obese IGT	Obese T2DM	P
n (men/women)	35 (14/21)	17 (5/12)	12 (4/8)	
Age (years)	48.4 ± 11.6	47 ± 14.2	44 ± 11.1	0.7
BMI (kg/m²)	39.0 ± 1.6	40.2 ± 1.9	41.2 ± 1.6	0.7
Body fat (%)	40.2 ± 1.02	50.3 ± 1.5	52.1 ± 2.5	0.4
Fasting glucose (mg/dL)	86.6 ± 1.3	110.2 ± 2.1	213.1 ± 19.8	<0.001
Triglycerides (mg/dL)	114.7 ± 15.4	149 ± 17.2	200.7 ± 45.2	0.049
HDL-cholesterol (mg/dL)	56.9 ± 3.8	54.2 ± 4.2	47.2 ± 3.5	0.28
LDL-cholesterol (mg/dL)	106.1 ± 34.1	114 ± 8.8	124.9 ± 15.1	0.4
Fasting insulin (μU/mL)	12.3 ± 3.1	29.1 ± 4.7	30.2 ± 7.6	0.2 †
HOMA-IR	2.6 ± 0.7	8.2 ± 1.2	9.7 ± 1.3	0.09 †

BMI, body mass index; CRP, C-reactive protein. Data are mean ± SEM. Differences between groups were analyzed by one-way ANOVA followed by Tukey's *post hoc* tests. **P*<0.05 and ***P*<0.01 vs Lean. †*P*<0.05 and ††*P*<0.01 vs obese NGT. †††*P*<0.01 vs obese IGT. † these values are representative from only 13 subjects rather than the 64 subjects used for the other parameters.

Table 2. Correlations between visceral and subcutaneous GPR55 expression and selected metabolic parameters of subjects in cohort 1.

Visceral GPR55

	Men (n=25)		Women (n=30)	
	Pearson	p	Pearson	p
Weight	0.33	0.052	0.49	0.0024**
BMI	0.34	0.046*	0.42	0.0095**
Fat %	0.15	0.242	0.33	0.035*
Glucose	0.25	0.158	0.10	0.297
Insulin	0.42	0.045*	0.27	0.095
TGs	0.60	0.004**	-0.02	0.539
Total Chol.	-0.29	0.870	-0.10	0.694
LDL Chol.	-0.55	0.987	-0.08	0.671
HDL Chol.	-0.35	0.912	-0.04	0.588
Leptin	0.34	0.107	0.32	0.100
LPI	0.39	0.028*	0.20	0.130
HOMA-IR	0.28	0.11	0.35	0.02*

Subcutaneous GPR55

	Men (n=25)		Women (n=30)	
	Pearson	p	Pearson	p
Weight	0.27	0.118	-0.09	0.684
BMI	-0.06	0.61	-0.05	0.600
Fat %	0.35	0.062	-0.20	0.846
Glucose	0.17	0.257	0.31	0.080
Insulin	-0.34	0.869	0.04	0.419
TGs	0.003	0.496	-0.07	0.622
Total Chol.	0.31	0.147	-0.14	0.728
LDL Chol.	0.36	0.128	-0.07	0.622
HDL Chol.	-0.07	0.595	-0.31	0.906
Leptin	-0.13	0.68	-0.10	0.661
LPI	-0.21	0.792	-0.21	0.846
HOMA-IR	-0.19	0.73	0.08	0.35

Table 3. Correlations between visceral and subcutaneous CB1 expression and selected metabolic parameters of subjects in cohort 1.

Visceral CB1

	Men (n=25)		Women (n=30)	
	Pearson	p	Pearson	p
Weight	0.13	0.269	0.22	0.112
BMI	0.24	0.116	0.17	0.179
Fat %	0.18	0.200	0.36	0.022*
Glucose	0.51	0.014*	0.06	0.372
Insulin	0.21	0.215	-0.13	0.743
TGs	0.29	0.128	0.02	0.448
Total Chol.	-0.37	0.931	0.07	0.361
LDL Chol.	-0.27	0.849	0.03	0.432
HDL Chol.	-0.17	0.740	0.18	0.173
Leptin	0.55	0.014*	0.13	0.309

Subcutaneous CB1

	Men (n=25)		Women (n=30)	
	Pearson	p	Pearson	p
Weight	-0.13	0.723	0.40	0.017*
BMI	-0.23	0.852	0.46	0.007**
Fat %	-0.05	0.587	0.06	0.381
Glucose	0.05	0.420	0.31	0.083
Insulin	0.42	0.067	-0.14	0.725
TGs	-0.02	0.530	0.34	0.066
Total Chol.	0.27	0.190	-0.10	0.666
LDL Chol.	0.34	0.141	-0.03	0.562
HDL Chol.	-0.09	0.619	-0.62	0.998
Leptin	-0.17	0.725	0.48	0.017*

Table 4. Correlations between visceral GPR55 expression and selected metabolic parameters of subjects in cohort 2.

	Men (n=20)		Women (n=44)	
	Pearson	p	Pearson	p
Weight	0,26	0.27	0.39	0.01*
BMI	0.29	0.21	0.31	0.03*
Fat %	0.3	0.19	0.32	0.03*
Glucose	0.32	0.17	0.07	0.64
Insulin	0.46	0.3	-0.03	0.9
TGs	0.15	0.5	-0.03	0.86
Total Chol.	-0.06	0.82	-0.07	0.64
LDL Chol.	-0.09	0.75	-0.27	0.057
HOMA-IR	0.43	0.33	-0.03	0.85

Table 5. Correlations between circulating LPI levels and selected metabolic parameters of subjects in cohort 1.

	Men (n=48)		Women (n=30)	
	Pearson	p	Pearson	p
Weight	-0.08	0.72	0.32	0.039*
BMI	-0.02	0.57	0.31	0.048*
Fat %	0.10	0.29	0.48	0.0037**
Glucose	-0.34	0.97	-0.032	0.56
Insulin	-0.12	0.76	0.09	0.33
TGs	-0.15	0.77	0.12	0.26
Total Chol.	-0.03	0.56	0.22	0.13
LDL Chol.	-0.14	0.75	0.34	0.042*
HDL Chol.	0.19	0.14	0.06	0.67
Leptin	0.02	0.44	0.24	0.14

Figure legends

Figure 1. mRNA expression of GPR55 (A), CB1 (B) and CB2 (C) in visceral adipose tissue obtained from lean and obese subjects in cohort 1. mRNA expression of *GPR55* (D) and CB1 (E) in subcutaneous adipose tissue obtained from lean and obese subjects in cohort 1. mRNA expression of GPR55 (F) in visceral adipose tissue obtained from lean and obese subjects in cohort 2. Protein levels of GPR55 (G) in visceral adipose tissue obtained from lean and obese subjects in cohort 2. Protein levels of GPR55 in the three different groups of obese patients (H). mRNA expression of GPR55 in the visceral and subcutaneous fat from the same obese patients (I). Protein levels of GPR55 in the visceral and subcutaneous fat from the same obese patients (J). mRNA expression of CB1 in the visceral and subcutaneous fat from the same obese patients (K). Obese subjects were subclassified as normoglycemic (NGT), impaired glucose tolerant (IGT) and type 2 diabetes (T2D). The relative amounts of mRNA were normalized to the value of NGT. # P<0.05, ## P<0.01, ### P<0.001 vs lean subjects; * P<0.05, **P<0.01 vs NGT

Figure 2. Correlation between visceral adipose tissue *GPR55* and body weight (A), body mass index (B), and circulating LPI (C) in individuals from cohort 1. For the cohort 1 we performed the correlations using only obese individuals and the cut-off value as a diagnose of obesity was BMI > 30 kg/m². Correlation between visceral adipose tissue *GPR55* and body weight (D) and body mass index (E) in individuals from cohort 2.

Figure 3. Circulating levels of total LPI (A), 16:0 LPI (B), 18:0 LPI (C), and 20:4 LPI (D) in the plasma obtained from lean and obese subjects in cohort 1. Correlation between circulating levels (plasma obtained from a subset of individuals from cohort 1) of total LPI and body weight (E), body mass index (F), and fat percentage (G) in women. Circulating levels of total LPI (H), 16:0 LPI (I), 18:0 LPI (J), and 20:4 LPI (K) in the plasma obtained from men and women in cohort 1. * P<0.05, ** P<0.01, ***P<0.001.

Figure 4. *Ex-vivo* effects of LPI (1 μ M and 10 μ M) on FASN (A), ACC (B), PPAR γ (C), leptin (D), Adipoq (E) and GPR55 (F) in visceral adipose tissue explants. *Ex vivo* effects of LPI on FASN (G), ACC (H), PPARG (I), leptin (J), ADIPOQ (K) and GPR55 (L) in subcutaneous adipose tissue explants. *P<0.05, ** P<0.01,

Figure 5. Representative profiles of the effects of LPI (5 μ M) on intracellular calcium levels ($[Ca^{2+}]_i$) in cultured differentiated human adipocytes obtained from visceral (A) and subcutaneous (C) fat. The arrows indicate the time of addition of LPI. A Fura-2 dual-wavelength fluorescence imaging system was used to measure $[Ca^{2+}]_i$ as described in Materials and Methods. Quantitation of $[Ca^{2+}]_i$ dynamics in differentiated adipocytes of VAT (B) and SAT (D) responsive to LPI (46 out of 95 cells and 29 out of 119 cells for VAT and SAT, respectively). Three independent experiments were conducted for both SAT and VAT adipocytes .

Figure 1

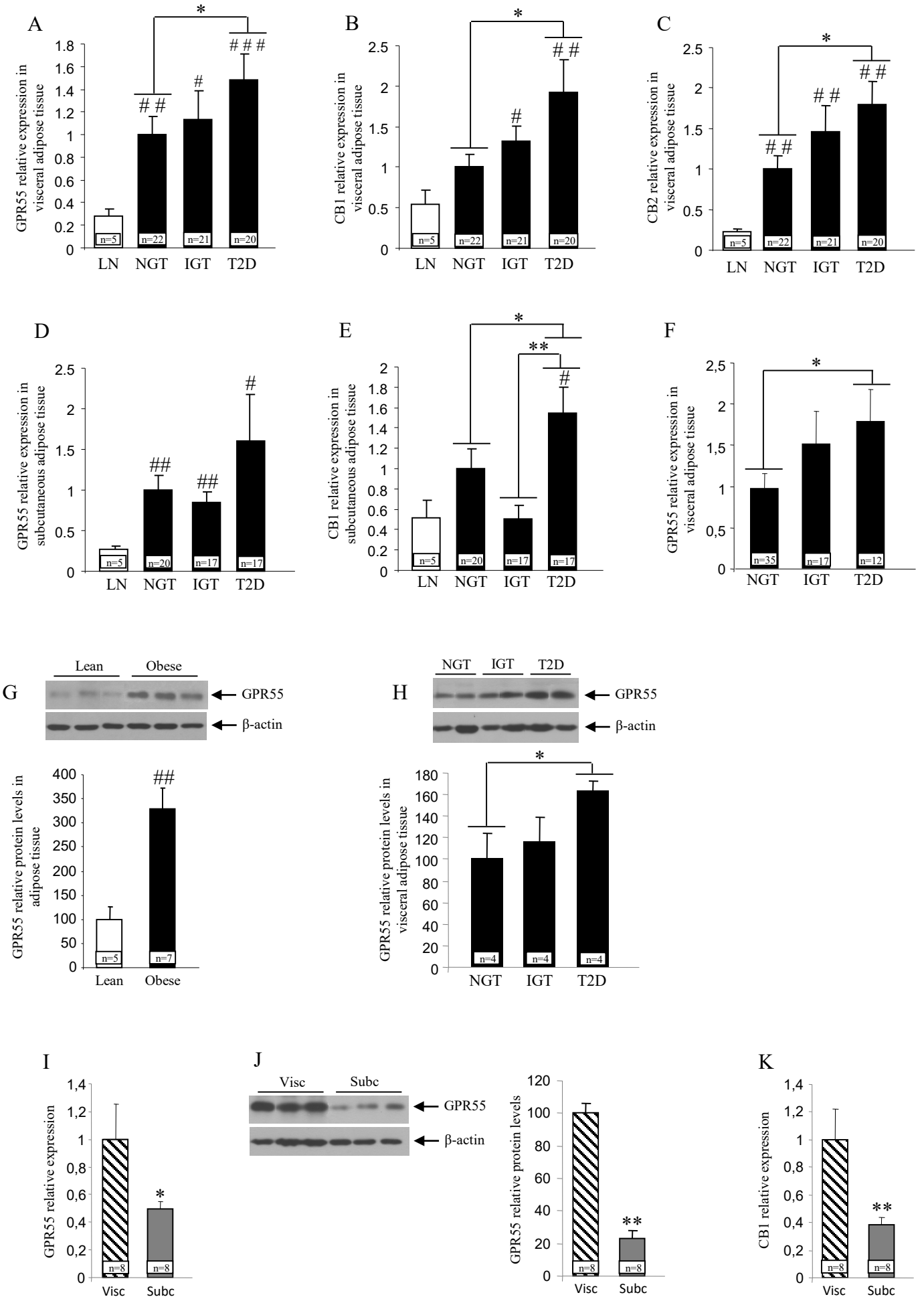


Figure 2

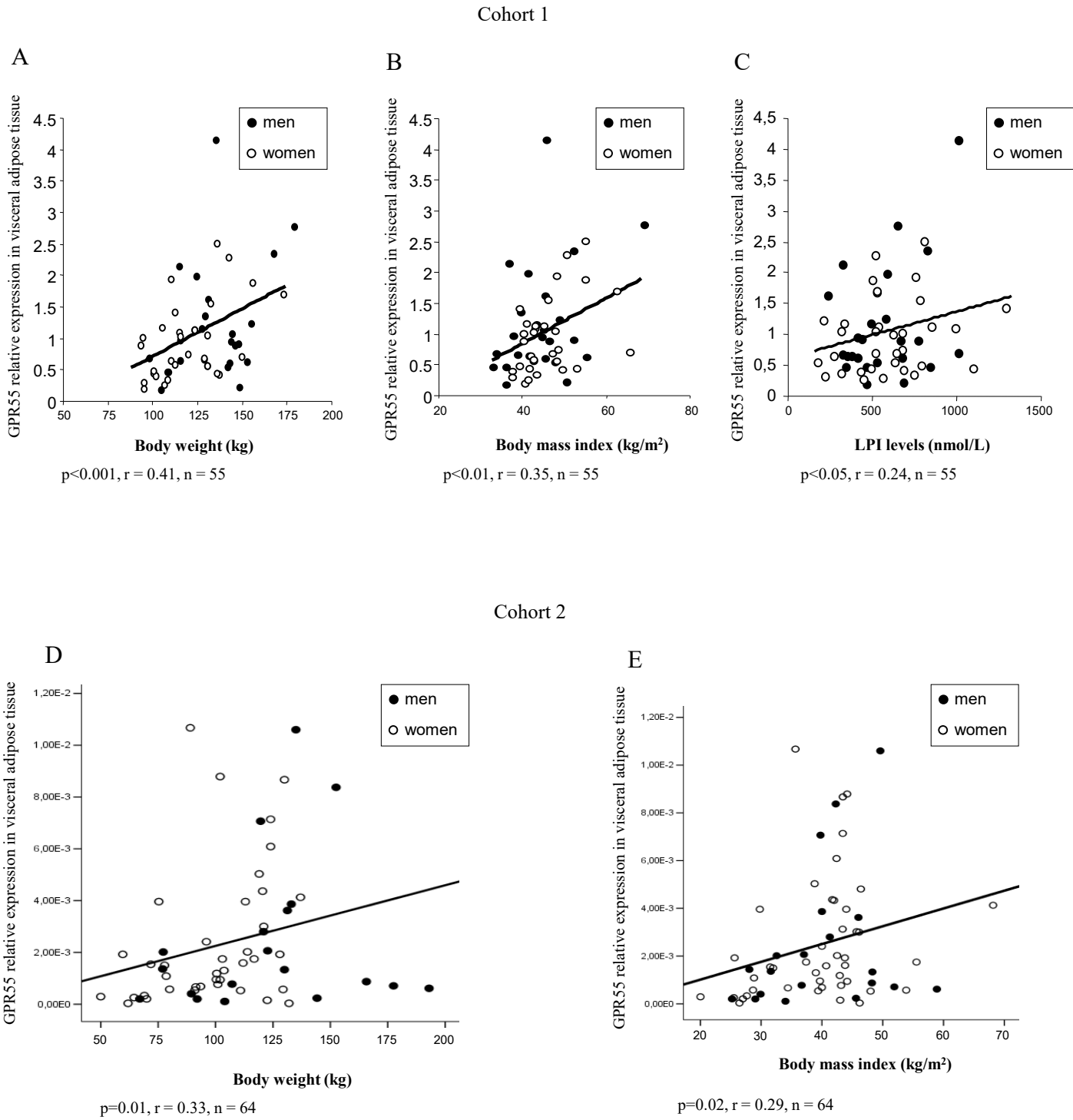


Figure 3

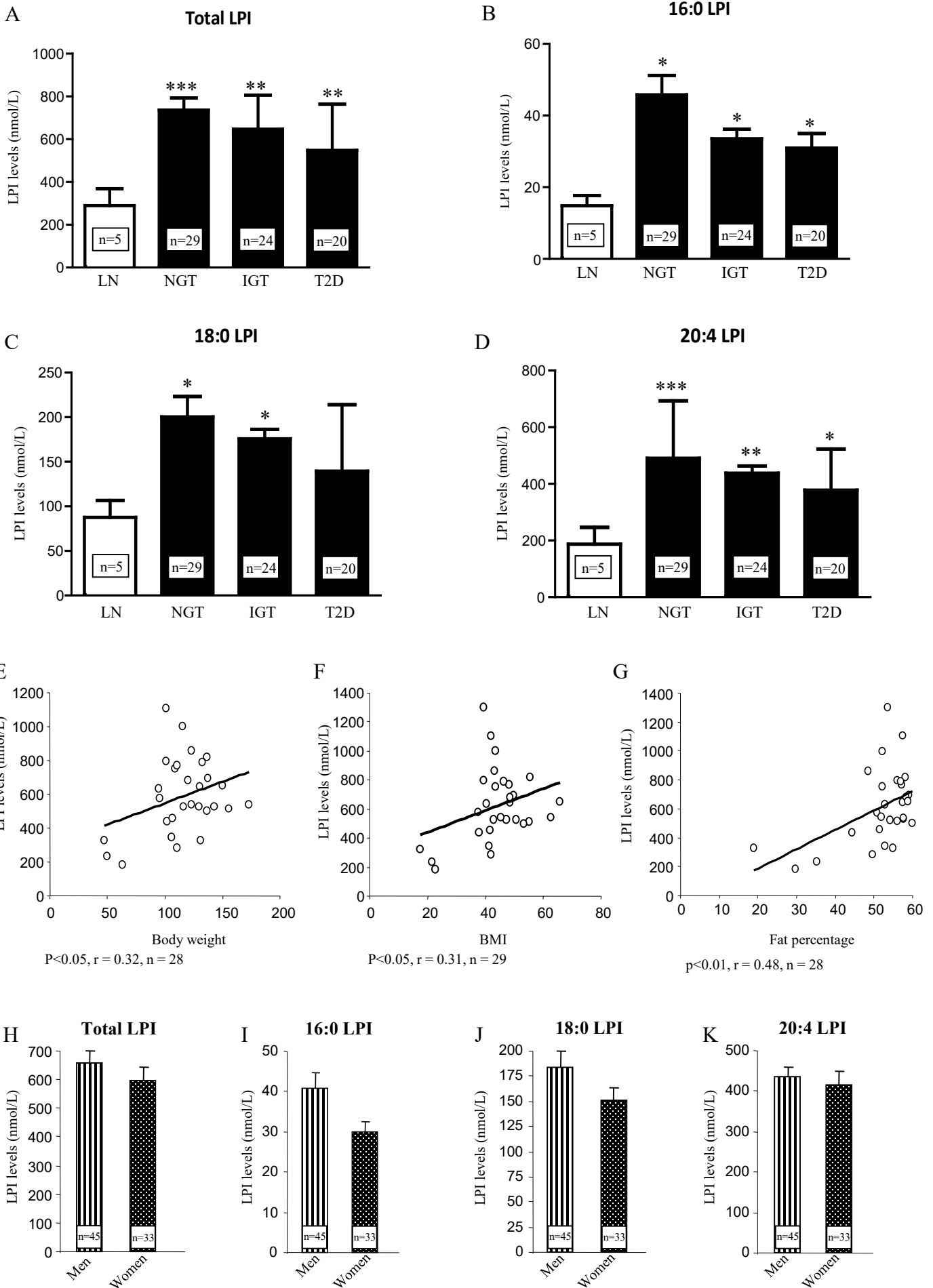


Figure 4

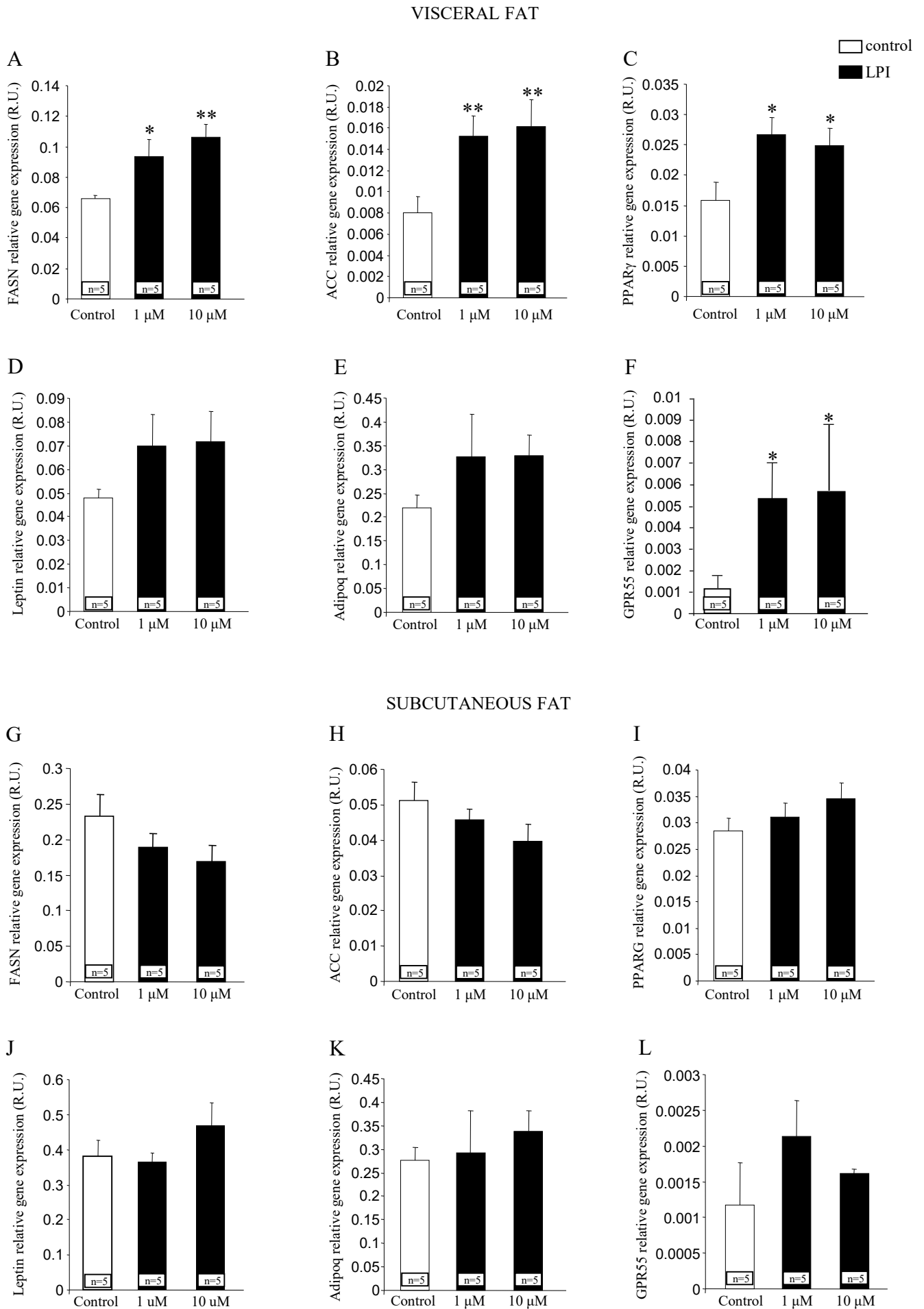
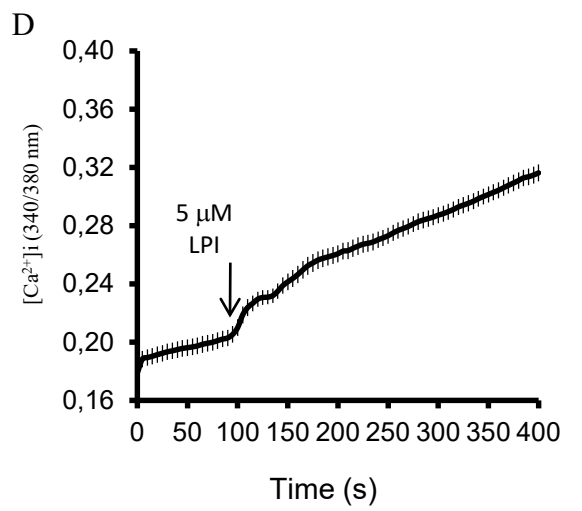
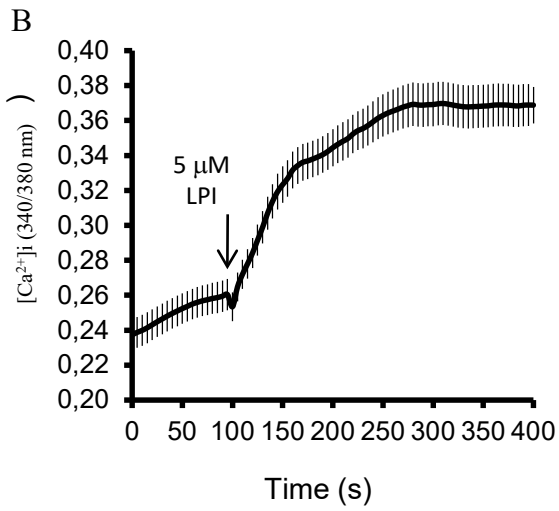
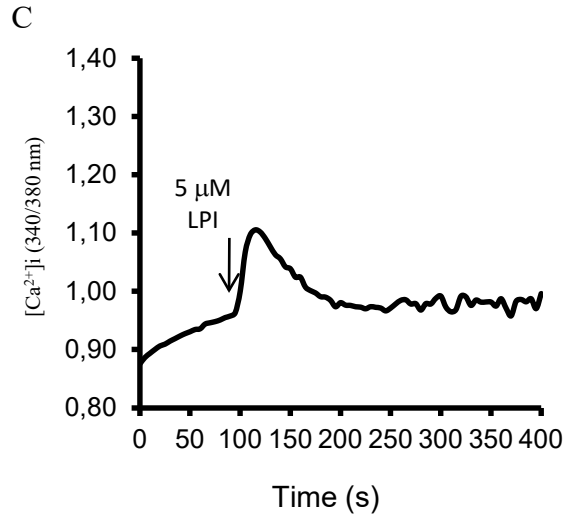
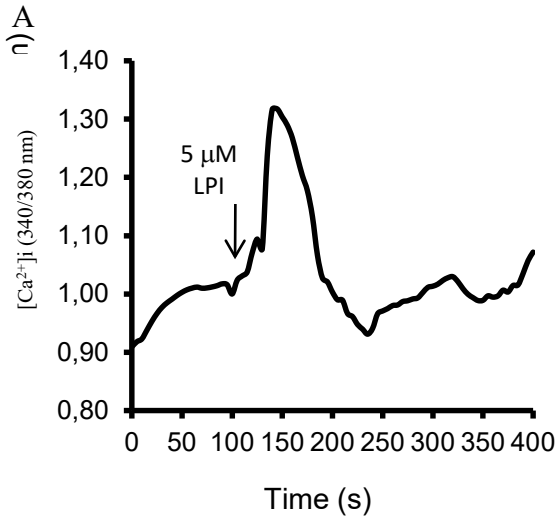


Figure 5



Supplemental information

Supplemental Research Design and Methods

Animals

Male Sprague–Dawley rats (Bred in the Animalario General USC; Santiago de Compostela, Spain) fed on low fat or high fat diet (reference #: D12451 and D12450B respectively, Research Diets, NJ, US) and male leptin-deficient mice (ob/ob) (8 weeks old, purchased from Charles River, Barcelona, Spain) were used. Animals were housed under conditions of controlled illumination (12:12-h light/dark cycle), humidity, and temperature. 8 animals per group were used in each experimental protocol. The animals were sacrificed by decapitation in a room separate from other experimental animals in the afternoon (16:00–17:00 h). Visceral WAT was then collected and frozen at -80°C until mRNA analysis. All experimental procedures in this study were reviewed and approved by the Ethics Committee of the University of Santiago de Compostela in accordance with our institutional guidelines and the European Union normative for the care and use of experimental animals.

Effect of LPI on adipocyte differentiation of 3T3-L1 cells

The 3T3-L1 adipocyte differentiation procedure was carried out in the presence or absence of LPI (1 and 10 μM) during 10 days. During this period, treatment was renewed every two days. At day 10, cells were fixed in paraformaldehyde (4%) for 15 min, thoroughly washed in 60% isopropanol and incubated in Oil Red O solution (Sigma) for 30 min. After washing out the excess of dye with H_2O_2 , plates were placed in a bright-field microscope and snap-shots of random fields were captured using a 10X objective. Afterwards, Oil Red O was eluted by incubating cells with 100% isopropanol for 10 min and optical density measured at 500 nm to estimate dye incorporation.

Supplemental Figure Legends

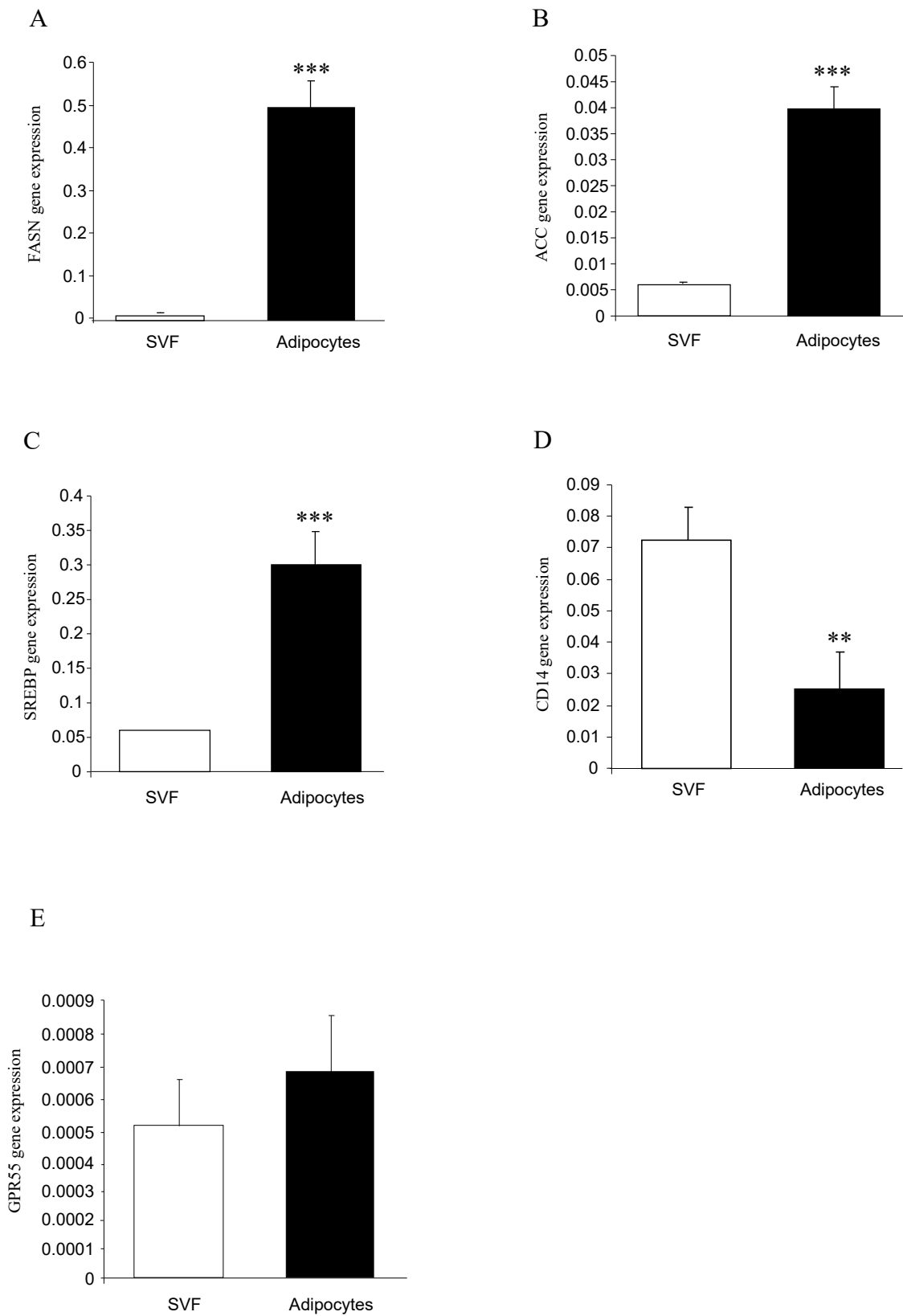
Supplemental figure 1. mRNA levels of *FASN* (A), *ACC* (B), *SREBP* (C), *CD14* (D), and *GPR55* (E) in the stromal vascular fraction (SVF) and adipocytes from humans. ** P<0.01, *** P<0.001.

Supplemental figure 2. *GPR55* mRNA expression in liver obtained from obese subjects of cohort 1. Obese subjects were subclassified as normoglycemic (NGT), impaired glucose tolerant (IGT) and type 2 diabetes (T2D).

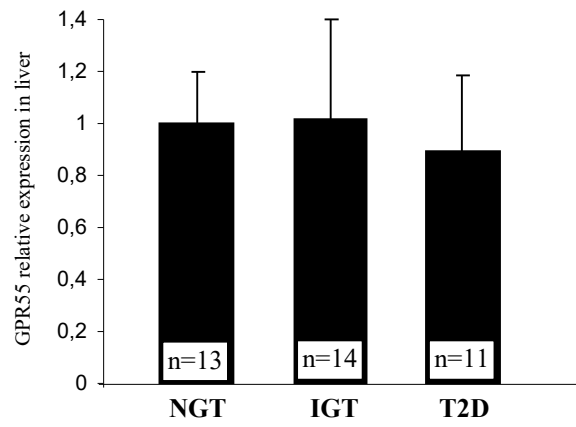
Supplemental figure 3. Representative bright-field images of 3T3-L1 cells differentiated to adipocytes during 10 days in the absence (left panel) or presence of 1 μ M and 10 μ M LPI (right panels) and stained with Oil Red O (A). Fluorimetric quantification of Oil Red O staining in 3T3-L1 cells at day 10 of differentiation into adipocytes in the absence or presence of 1 μ M and 10 μ M LPI (B). Values are represented as mean \pm SEM of 3 independent experiments.

Supplemental figure 4. *GPR55* mRNA expression in the WAT of ob/ob vs wild type mice (A), and rats fed on low fat diet vs high fat diet (B). *GPR55* protein levels in the WAT of ob/ob vs wild type mice (C), and rats fed on low fat diet vs high fat diet (D).

Supplementary figure 1

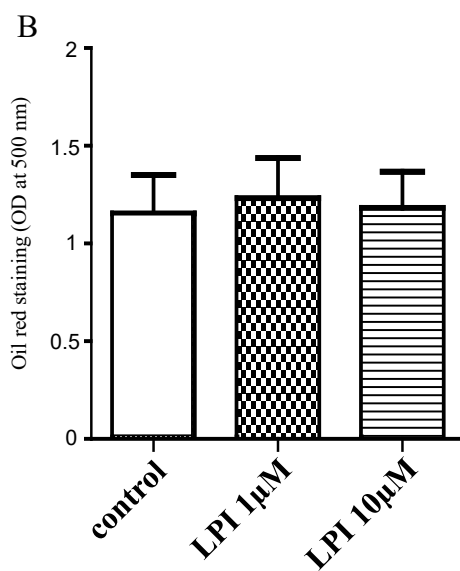
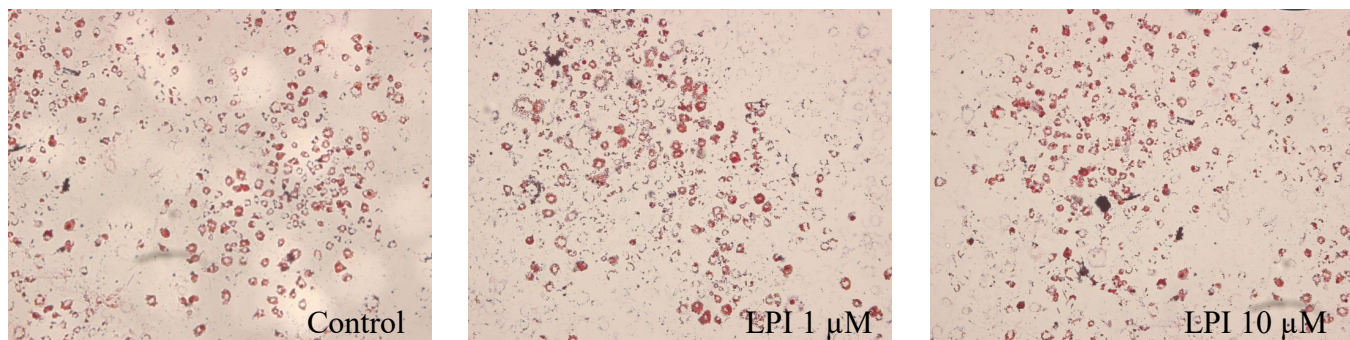


Supplementary figure 2

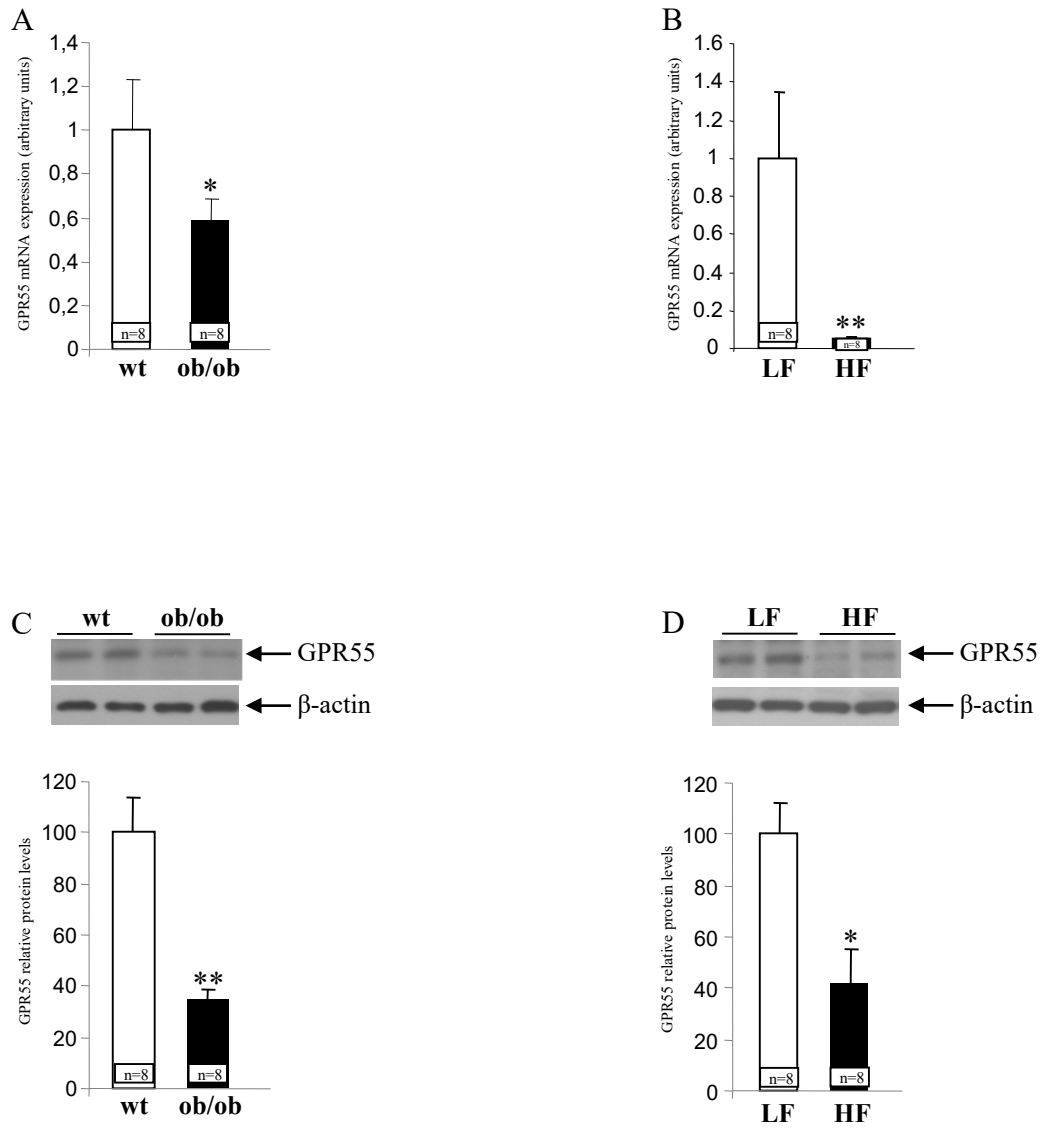


Supplementary figure 3

A



Supplementary figure 4



Supplementary table 1. Anthropometric and analytical characteristics of subjects of cohort 1 used for the determination of circulating LPI.

	Lean	Obese NGT	Obese IGT	Obese T2DM	P
N (men/women)	5 (2/3)	29 (11/18)	24 (12/12)	20 (8/12)	
Age (years)	38 ± 4	36 ± 2	42 ± 2	45 ± 2 ^{††}	0.053
BMI (kg/m²)	21.3 ± 1.1	43.1 ± 1.2 ^{**}	45.5 ± 1.1 ^{**}	48.9 ± 2.3 ^{**}	<0.001
Body fat (%)	26.5 ± 2.8	48.7 ± 1.6 ^{**}	53.3 ± 1.0 ^{**}	52.6 ± 1.3 ^{**}	<0.001
Fasting glucose (mg/dL)	86.8 ± 3.5	89.0 ± 1.9	104.7 ± 2.2	151.3 ± 15.8 ^{**,††,##}	<0.001
Fasting insulin (μU/mL)	8.2 ± 1.7	17.0 ± 1.6	18.5 ± 2.3	21.1 ± 2.9	0.070
Triglycerides (mg/dL)	68 ± 11	101 ± 9	140 ± 25	204 ± 53	0.069
Cholesterol (mg/dL)	192 ± 10	181 ± 8	209 ± 9	204 ± 8	0.081
LDL-cholesterol (mg/dL)	118 ± 10	119 ± 6	131 ± 8	130 ± 8	0.562
HDL-cholesterol (mg/dL)	58 ± 2	41 ± 2 [*]	50 ± 2 [†]	43 ± 2 [*]	<0.01
Leptin (ng/mL)	7.8 ± 1.5	51.0 ± 5.8 [*]	58.9 ± 6.5 ^{**}	68.3 ± 9.6 ^{**}	<0.01
CRP (mg/L)	1.8 ± 0.3	6.8 ± 1.4	13.1 ± 2.4 [*]	9.3 ± 1.9	0.016

BMI, body mass index; CRP, C-reactive protein. Data are mean ± SEM. Differences between groups were analyzed by one-way ANOVA followed by Tukey's *post hoc* tests. **P*<0.05 and ***P*<0.01 vs Lean. †*P*<0.05 and ††*P*<0.01 vs obese NGT. ##*P*<0.01 vs obese IGT.

Supplementary table 2. Primer sequences used for real-time PCR.

Gene	Accession	Sequence	
<i>GPR55</i>	NM_005683.3	Forward	5'- GCA TGG ATC ACC CCA AGT TTC -3'
		Reverse	5'- TCA TCA ACA CCC CAC TCA GTC A -3'
		Probe	FAM-5'- CCG TGC CCG TGA GAA GAC TGC AAA-3'- TAMRA
<i>CB1</i>	AY995204.1	Forward	5'- AGG ACC TGC GAC ACG CTT T -3'
		Reverse	5'- CGA GTC CCC CAT GCT GTT ATC -3'
		Probe	FAM-5'- TGT TTC CCT CTT GTG AAG GCA CTG CG-3'- TAMRA
<i>CB2</i>	NM_001841.2	Forward	5'- CCTGGGAGAGGACAGAAAACAA -3'
		Reverse	5'- TGGGCCCTTCAGATTCCA -3'
		Probe	FAM-5'- CAGCCACCCACAACACAACCCAAA-3'-TAMRA
<i>FASN</i>	NM_004104.4	Applied Biosystems, reference Hs00188012_m1	
<i>ACCA</i>	AY237919.1	Applied Biosystems, reference Hs00167385_m1	
<i>SREBP</i>	NM_001005291.2	Applied Biosystems, reference SREBP1: Hs00231674_m1	
<i>CD14</i>	M86511.1	Applied Biosystems, reference Hs00169122_g1	
<i>Adiponectin</i>	EU420013.1	Applied Biosystems, reference Hs00605917_m1	
<i>PPARG</i>	L40904.2	Applied Biosystems, reference Hs00234592_m1	
<i>Leptin</i>	NM_000230.2	Applied Biosystems, reference Hs00174877_m1	
<i>Cyclophilin A</i>	NM_021130.3	Applied Biosystems, reference 4333763	

Supplementary table 3. Multivariate linear regression analyses with GPR55 gene expression in VAT as dependent variable.

Cohort 1

Men GPR55 mRNA levels				
	<i>Visceral adipose tissue</i>		<i>Subcutaneous adipose tissue</i>	
	$r^2=0.358; P=0.043$		$r^2=-0.049; P=0.549$	
	β	<i>P</i>	β	<i>P</i>
Age	-0.07	0.778	0.37	0.70
BMI	0.50	0.020	0.35	0.42
Triglycerides	1.07	0.025	1.02	0.37
Total-cholesterol	-0.34	0.188	-0.12	0.89
HOMA	-0.71	0.114	-0.98	0.26

Women GPR55 mRNA levels				
	<i>Visceral adipose tissue</i>		<i>Subcutaneous adipose tissue</i>	
	$r^2=0.207; P=0.026$		$r^2=-0.098; P=0.771$	
	β	<i>P</i>	β	<i>P</i>
Age	0.03	0.856	0.19	0.459
BMI	0.42	0.018	0.10	0.698
HOMA	2.58	0.134	0.20	0.411

Cohort 2

Men GPR55 mRNA levels				
	<i>Visceral adipose tissue</i>		<i>Subcutaneous adipose tissue</i>	
	$r^2=-0.018; P=0.46$		$r^2=0.084; P=0.28$	
	β	<i>P</i>	β	<i>P</i>
Age	0.12	0.653	0.18	0.566
BMI	0.32	0.277	0.63	0.077
Type 2 diabetes	0.19	0.445	-0.28	0.325

Women GPR55 mRNA levels				
	<i>Visceral adipose tissue</i>		<i>Subcutaneous adipose tissue</i>	
	$r^2=0.054; P=0.16$		$r^2=0.066 P=0.089$	
	β	<i>P</i>	β	<i>P</i>
Age	0.009	0.951	-0.078	0.563
BMI	0.331	0.032	0.292	0.036
Type 2 diabetes	0.080	0.599	-0.183	0.184

Beta is the standardized regression coefficient, which allows evaluating the relative significance of the each independent variable in multiple linear regression analyses. **Adjusted R square** express the percentage of the variance explained by the independent variables in the different models (i.e., 0.50 is 50%).